Published in final edited form as:
Lab Chip. 2013 May 7; 13(9): 1810–1816. doi:10.1039/c3lc50076d.

Miniature Grating for Spectrally-Encoded Endoscopy

Dongkyun Kang[a], **Ramses V. Martinez**[b], **George M. Whitesides**[b,c], and **Guillermo J. Tearney**[a,d,e]

Guillermo J. Tearney: tearney@helix.mgh.harvard.edu

[a]Harvard Medical School and Wellman Center for Photomedicine, Massachusetts General Hospital, 55 Fruit Street, Boston, MA 02114, USA

[b]Department of Chemistry and Chemical Biology, Harvard University, 12 Oxford Street, Cambridge, MA 02138, USA

[c]Wyss Institute for Biologically Inspired Engineering, Harvard University, 60 Oxford Street, Cambridge, MA 02138, USA

[d]Harvard-MIT Division of Health Sciences and Technology, 77 Massachusetts Avenue, Cambridge, MA 02139, USA

[e]Department of Pathology, Harvard Medical School and Massachusetts General Hospital, 55 Fruit Street, Boston, MA 02114, USA

Abstract

Spectrally-encoded endoscopy (SEE) is an ultraminiature endoscopy technology that acquires high-definition images of internal organs through a sub-mm endoscopic probe. In SEE, a grating at the tip of the imaging optics diffracts the broadband light into multiple beams, where each beam with a distinctive wavelength is illuminated on a unique transverse location of the tissue. By encoding one transverse coordinate with the wavelength, SEE can image a line of the tissue at a time without using any beam scanning devices. This feature of the SEE technology allows the SEE probe to be miniaturized to sub-mm dimensions. While previous studies have shown that SEE has the potential to be utilized for various clinical imaging applications, the translation of SEE for medicine has been hampered by challenges in fabricating the miniature grating inherent to SEE probes. This paper describes a new fabrication method for SEE probes. The new method uses a soft lithographic approach to pattern a high-aspect-ratio grating at the tip of the miniature imaging optics. Using this technique, we have constructed a 500-μm-diameter SEE probe. The miniature grating at the tip of the probe had a measured diffraction efficiency of 75%. The new SEE probe was used to image a human finger and formalin fixed mouse embryos, demonstrating the capability of this device to visualize key anatomic features of tissues with high image contrast. In addition to providing high quality imaging SEE optics, the soft lithography method allows cost-effective and reliable fabrication of these miniature endoscopes, which will facilitate the clinical translation of SEE technology.

Introduction

Miniature endoscopy, where images are acquired through an endoscopic probe with a diameter smaller than 1 mm, has a potential to improve patient care by minimizing the risk and discomfort associated with the insertion of the probe. Fiber bundle-based miniature endoscopes have been utilized for various clinical applications, including fetal surgery,[1, 2] angioscopy,[3, 4] bronchoscopy,[5] and ductoscopy.[6] Recently, a miniature endoscope using a

Correspondence to: Guillermo J. Tearney, tearney@helix.mgh.harvard.edu.

small-size imaging sensor has been developed (Medigus; diameter = 1.2 mm; effective pixels = 49,280) for laparoscopic surgery and colonoscopy.[7] Single-fiber miniature endoscopes using miniature piezoelectric actuators also provide high-quality images of human tissues.[8, 9]

Spectrally encoded endoscopy (SEE) is an endoscopic technology that replaces a beam scanning device with a miniature diffraction grating to minimize the probe size.[10] In an SEE probe, broadband light is delivered by a fiber and focused by a miniature lens. A diffraction grating, which is positioned after the miniature lens, disperses the broadband light into multiple beams with different wavelengths (colors). Each color illuminates tissue in a different direction from the end of the fiber, and thus encodes light reflected from tissue in a given transverse coordinate by wavelength. A line image of the tissue is acquired by analyzing the light reflected from the tissue and returned by the fiber, by spectral frequency. The other transverse coordinate, which is typically perpendicular to the spectrally-encoded coordinate, is scanned by rotating the SEE probe by a motor that is located outside of the patient. Since line images of the tissue are acquired without using any beam scanning devices, the SEE probe can be made very small. When incorporated into the sample arm of an interferometer, the SEE probe can also acquire three-dimensional information from the tissue[11-13] and can provide information regarding the flow of blood.[14] Previously, we have demonstrated a 350-μm-diameter SEE probe, and carried out *in vivo* laparoscopic imaging of an animal model.[15]

Fabrication of the miniature grating at the tip of the SEE probe has been one of the main challenges in the development of the SEE technology. For the original demonstration of this device,[15] we fabricated miniature gratings by polishing a stack of glass rods at an angle, depositing a holographic grating pattern on the glass rod stack, and separating the glass rods.[16] Although we successfully fabricated 350-μm SEE probes, the fabrication method had three important limitations: i) The procedure for recording the holographic grating pattern required a special facility with very low vibration and thermal variation, which increased the fabrication cost. ii) The grating pattern on the glass rod often became damaged during the separation procedure. iii) Handling of the miniature grating was challenging, especially when the grating was precisely aligned with the imaging optics.

More recently, a new laser cutting technology for fabricating miniature gratings has been reported.[17] In this method, a pulsed laser beam was focused on an etched diffraction grating (Ibsen Photonics; material = fused silica; size = 20 mm by 20 mm by 0.65 mm), ablating the grating material at the focal point. The grating was then translated relative to the stationary laser beam to generate an elliptical laser cut. Then the back surface of the cut grating was polished to make it perpendicular to the optical axis. A 500-μm-diameter grating with high diffraction efficiency, 75%, was constructed with this approach. This laser cutting procedure, however, generates cracks around the edge of the miniature grating, around 40 μm wide,[17] making it difficult to reduce the grating size further. Moreover, handling of the miniature grating (diameter = 500 μm; thickness = 650 μm) can be challenging during the polishing and alignment procedures.

Replica molding is a form of soft lithography that uses elastomeric stamps to relief patterns on a master stamp to form patterns of polymeric materials on a surface through conformal contact. Polydimethylsiloxane (PDMS) has been widely used as a stamp in replica molding of microscale features over relatively large areas.[18] The low Young's modulus of PDMS (1.84 MPa), however, limits its use in the replication of high-aspect-ratio features or features smaller than 250 nm. The resolution of molding is limited, in principle, by the molecular graininess of matter and the rigidity of the mold and the material being molded. To

overcome the limitations of PDMS on replica molding caused by its low rigidity, other formulations of PDMS have been used.

Elhadj et al. demonstrated replication of elementary steps 3-5 Å in height that define the minimum separation between molecular layers in the lattices of the ionic crystals potassium dihydrogen phosphate and calcite, using an *h*-PDMS mold (Young's modulus = 9.7 MPa).[19] Rogers and co-workers demonstrated molecular-scale resolution by replicating the shapes of single-walled carbon nanotubes in polyurethane using an *h*-PDMS/PDMS stamp. This composite stamp combines the advantages of both a more rigid layer (to achieve high-resolution-pattern transfer) and a more flexible support (to enable conformal contact with a surface without external pressure).[20] *h*-PDMS/PDMS stamps have also been used for replicating very high-aspect-ratio features. The Aizenberg laboratory has demonstrated the replication of large (> 1 cm^2) arrays of high-aspect-ratio epoxy nanoposts (d = 250 nm and h =8 μm).[21]

This paper describes a new method of fabricating miniature SEE probes using a soft lithographic replication process. We built an *h*-PDMS/PDMS composite elastomeric stamp with a high-aspect ratio grating pattern. We then fabricated a miniature grating at the tip of the imaging optics by replica molding the grating pattern on the elastomeric stamp. A 500-μm-diameter dual-channel SEE probe was made with the new method. The grating profile at the tip of the SEE probe was evaluated, and the diffraction performance tested. Various samples were imaged to test the imaging performance, including the United States Air Force (USAF) resolution target, human fingers, and mouse embryos.

Methods

Design of the SEE system and probe

Figure 1a shows a schematic diagram of the SEE system. Light from a broadband source (SC400-6, Fianium; spectral bandwidth = 400-2400 nm; spectral power density = 3 mW/nm) was coupled into a SEE probe through the core of an illumination fiber (SMM900, Fibercore; core diameter = 3.71 μm; core numerical aperture (NA) = 0.19). Light from the SEE probe illuminated the sample, and light reflected from the sample was collected through a second fiber (FVP100110125, Polymicro; core diameter = 100 μm; polyimide coating diameter = 125 μm; NA = 0.22). The second fiber, termed detection fiber, was connected to a spectrometer, comprising a collimation lens (focal length = 100 mm), a diffraction grating (groove density = 1200 lines/mm), a focusing lens (focal length = 50 mm) and a line-scan camera (Sprint 2048-140km, Basler). The spectrum of the detected light, which is also the line image of the sample, was acquired by the spectrometer at a rate of 5 kHz. In order to acquire two-dimensional images, the SEE probe was rotated back and forth by a galvo scanner (6220H, Cambridge Technology) using a sawtooth pattern at a rate of 10 Hz.

Figure 1b illustrates the detailed schematic of the SEE probe. Light from the illumination fiber was focused by a gradient index (GRIN) rod lens (LFRL-050-023-20, GRINtech; diameter = 500 μm). A grating (groove density = 1379 lines/mm) at the tip of a 500-μm spacer diffracted the light from the GRIN lens. Each wavelength was diffracted at a unique angle and subsequently illuminated a distinct angular cone on the sample. For instance, a longer wavelength (red beam in Fig. 1b) is diffracted at a higher angle and focused on the transverse position x_1, while a shorter wavelength (blue beam in Fig. 1b) is diffracted at a smaller angle and focused on the position x_2. The angle of the grating relative to the optical axis was set as Littrow's angle at 532 nm to maximize the intensity of the +1st order beam. Other diffraction orders had significantly lower intensities than that of the +1st order, and therefore the detected signal was generated mainly by the +1st order. The field angle

achieved by diffraction was 28.6° for an optical spectrum that ranged between 485-789 nm. The number of resolvable points was calculated to be 275, which provided 550 effective pixels per line (Nyquist sampling). Light reflected from the sample was collected by the detection fiber. The detection fiber also had the grating pattern at the tip in order to make the propagation angle of the reflected light in the detection fiber fall within the acceptance angle of the detection fiber. The lateral surface of the GRIN lens was polished by 125 μm to fit the detection fiber along the same axis. The total diameter of the imaging optics was 500 μm.

Fabrication of the Two-Layer Elastomeric Stamp

We used a fused silica diffraction grating (VIS spectrometer grating, Ibsen Photonics; groove pitch = 725 nm; groove depth = 1 μm; substrate thickness = 625 μm; grating area = 13.5 mm by 12.5 mm) as the master for soft replica molding. We functionalized this master by placing the master in a Petri dish and then in a desiccator. Another Petri dish containing a few drops (100 ~μL) of tridecafluoro-1,1,2,2-tetrahydrooctyl-1-trichlorosilane (TFOCS, United Chemical Technology, cat. no. 6H-9283) was also placed in the same desiccator. We connected the desiccator to the vacuum line of the fume hood and evacuated the air from the desiccator until the pressure reached ~36 Torr. Then the desiccator was disconnected from the vacuum line and sealed at ~36 Torr during five hours to allow TFOCS to vaporize and deposit as a monolayer on the master through siloxane bonding. The TFOCS vapor transformed the surface of a master from hydrophilic to hydrophobic.[18] This modification prevented the cured PDMS from adhering to the master. Once the modification was done, the master was ready to be used to fabricate multiple copies (at least 20) of PDMS-based stamps without additional surface treatment.

In order to prepare *h*-PDMS, we mixed 3.4 g of a vinyl PDMS prepolymer (VDT-731, Gelest Corp.), 18 μL of a Pt catalyst (platinum divinyltetramethyldisiloxane, SIP6831.1, Gelest Corp.), and one drop of a modulator (2,4,6,8-tetramethyl-tetravinylcyclotetrasiloxane, 87927, Sigma-Aldrich) and degassed for 1-2 minutes. We then gently stirred 1 g of a hydrosilane prepolymer (HMS-301, Gelest Corp.) into this mixture. Immediately (within 3 minutes), we spin-coated a thin layer (30-40 μm) of *h*-PDMS onto the functionalized master (1000 rpm, 40 seconds) and cured it for ten minutes at 70 °C. The *h*-PDMS was still slightly tacky after this curing procedure. We then poured a liquid pre-polymer layer (~ 3 mm) of Sylgard 184PDMS (s-PDMS, Dow Corning) onto the h-PDMS layer and cured it for two hours at 70 °C. We released the composite stamp from the surface by cutting and carefully peeling the stamp from the surface while still warm.

Fabrication of the SEE probe

We aligned the illumination fiber, GRIN lens, and spacer while monitoring the spot profile after the spacer. The gap between the illumination fiber and GRIN lens was adjusted to achieve a working distance of 15 mm. Once the alignment was completed, the GRIN lens, spacer and the illumination fiber were assembled together using UV curing epoxy (OG142-112, Epoxy technology). Then the detection fiber was aligned with the illumination optics and assembled using a black UV curing epoxy (OG147, Epoxy technology). The black UV curing epoxy absorbed any stray illumination light and prevented the stray light from being coupled to the detection fiber. A thin-wall heat shrink tubing (wall thickness = 25.4 μm) was placed on the imaging optics to provide additional mechanical integrity.

We then polished the distal tip of the imaging optics at an angle of 14.5°. A very thin layer (~15 μm) of another UV curing epoxy (OG603, Epoxy technology) was applied on the angle-polished surface of the imaging optics. We then mounted the composite elastomeric stamp on a three-axis precision translation stage and carefully placed the stamp into a contact with the UV curing epoxy. The surface of the elastomeric stamp was made parallel

to the angle-polished surface of the imaging optics. The elastomeric stamp was further aligned to form the UV curing epoxy into a circular profile that had the same diameter as the imaging optics. The epoxy was cured by a UV lamp (Blue Wave 75, Dymax) for 100 seconds. Once the epoxy was cured, the elastomeric stamp was carefully pulled away from the cured epoxy using the translation stage, leaving the miniature grating at the tip of the imaging optics. The refractive index of this UV curing epoxy was n = 1.47 at 589 nm, which was similar to that of the master grating at the same wavelength (n= 1.46). Use of an epoxy that has a refractive index similar to that of the master grating made it possible to achieve good diffraction efficiency for the miniature grating.

Results

Miniature grating fabrication

Figure 2a depicts a highly magnified photograph of the tip of the SEE probe. The central elliptical region at the distal tip of the SEE probe is green because the grating formed at the probe's tip diffracted the illumination light of the microscope system and preferentially directed the green light to the microscope camera at this particular viewing angle. The area of the green region indicated the area where the miniature grating was well formed. We have measured the green area and found that approximately 86% of the probe diameter along the long axis of the grating and 78% along the short axis showed the green diffraction pattern. A scanning electron microscope (SEM) image (Fig. 2b) of the SEE probe was acquired with a Zeiss Supra55 VP FESEM at 2 kV at a working distance of 6 mm. Before SEM imaging, the SEE probe was placed on a silicon wafer and sputter coated with Pt/Pd at 60 mA for 15–45 seconds. The high-magnification SEM image reveals the regular line pattern of the grating (Fig. 2c). The standard deviation of the groove pitch was measured. We first extracted a line profile of the SEM image of the miniature grating along the direction perpendicular to the groove direction by using ImageJ® (http://rsbweb.nih.gov/ij/). We then conducted the Fourier Transform (FT) of the line profile and measured the spatial frequency that had the maximum amplitude, f_{max}. The mean pitch of the grating in this line profile was calculated as $1/f_{max}$.[22] The grating pitches were measured for a total of 104 line profiles, and the standard deviation of the grating pitch was measured to be 1.2 % of the mean grating pitch.

The diffraction performance of the miniature grating was tested. The SEE probe generated the spectrally-encoded illumination pattern, which appears as a linear rainbow (Fig. 3). The diffraction efficiency of the +1st order, the intensity of the +1st order divided by the intensity of the input beam, was measured to be 75% for the beam diameter of 500 μm and the input wavelength of 532 nm. This diffraction efficiency is lower than that of the master grating, 85%. The grating diameter was smaller than the probe diameter, and therefore a portion of light was not diffracted, which reduced the diffraction efficiency. The difference of the refractive index between the master grating and the replicated grating might have also decreased the diffraction efficiency.

SEE imaging

The imaging characteristics of the SEE probe were tested, including the lateral resolution, number of resolvable points, and tissue imaging capability. The SEE probe was inserted into a modified 20-gauge needle (outer diameter = 0.9 mm; inner diameter = 0.6 mm). A 0.6 mm-by-1.2 mm elliptical opening was made on the needle wall for imaging and covered with a heat shrink tubing (wall thickness = 10 μm). The SEE probe was rotated back and forth over an angle of 40 degrees. A USAF 1951 resolution target was imaged to measure the lateral resolution and number of resolvable points. At the working distance of 10 mm, the lines at the group 2, element 6 (line width = 70 μm) were clearly resolved. When the resolution target was positioned at the working distance of 20 mm, the lines at the group 2,

element 2 (line width = 111 μm) were clearly resolved. The field widths were approximately 10 and 20 mm for the working distances of 10 and 20 mm, respectively. The number of resolvable points was calculated by dividing the field width by the line width of the smallest resolvable line pattern, and the number ranged from 142 to 180. The measured number of resolvable points was smaller than the expected number, 275. The effective light beam diameter for imaging was decreased to approximately 400 μm due to the lack of the grating pattern at the edge of the optics (Fig. 2a), reducing the number of resolvable points. Alignment errors during the fabrication of the illumination optics might have degraded the imaging resolution, which could also decrease the number of resolvable points.

A human finger was imaged with the SEE probe at various working distances (Fig. 4). Microscopy images of the same finger were taken, and the scale bars in Fig. 4 have been calibrated based on these microscopy images. The calibrated field width is 14 mm, 5.7 mm and 2.2 mm for the Fig. 4a, b, and c, respectively. In all three figures, details of the fingerprints are clearly visualized. This result shows that the SEE probe can image tissue clearly for a wide range of the working distances (i.e. has a good depth of field), which is a key requirement for endoscopic imaging devices. Mouse embryos were also imaged with the SEE probe. Mouse embryos were inside a polypropylene 50 ml tube, and the SEE imaging was conducted through an approximately 10 mm thick layer of 3.7% formaldehyde fixative solution. The SEE images (Fig. 5a, b, and c) enable the clear visualization of anatomic features of the embryo, including the head, eye (arrow), tail (asterisk) and paws with claws (dotted arrows), which are similar to those shown in the photo of the same animal (Fig. 5d).

Discussion

One of the key advantages of the new fabrication method is that SEE probes can be made with a low cost. Each elastomeric stamp (effective grating area = 13.5 mm by 12.5 mm) can be used to fabricate approximately 170 miniature gratings assuming that a 1 mm by 1 mm area of the stamp is needed for fabricating a 500-μm-diameter grating. Multiple elastomeric stamps can be made without damaging the master. The low cost makes it possible to fabricate cheap and disposable SEE probes, which can facilitate the clinical use of the technology.

It is also advantageous that the current fabrication method forms the miniature grating on the imaging optics as the last step. When the grating is not properly formed during the fabrication process or is damaged during the use, the tip of the SEE probe can be easily angle-polished by a very small amount (~20 μm) to remove the damaged grating. Following this corrective action, a new grating can then be fabricated on the same imaging optics. A procedure for handling and precisely aligning the miniature grating is not needed in the current method, which makes the fabrication process easier than would a method requiring alignment. The same grating fabrication method can be used for any imaging optics of a range of designs, regardless of the number and dimension of the optical components used.

Another merit of the current fabrication method is that the SEE probe size can be decreased further. A ultraminiature GRIN lens with a diameter of 80 μm is recently being developed from a GRIN lens company, GRINtech.[23] The current method can be used to make a grating at the tip of the 80-μm GRIN lens, which makes it possible to consider an ultraminiature SEE probe with a diameter that is smaller than 100 μm. We expect that the small diameter of the ultraminiature SEE probe will enable us to image internal tissues that are not currently accessible by any existing endoscopic imaging devices.

Even though there are many advantages to this soft lithography technique, we encountered some challenges. As discussed before, the grating pattern did not cover the entire aperture of

the probe optics. When the epoxy came in contact with the elastomeric stamp, the epoxy spread along the grooves by capillary action, forming an elliptical rather than a circular profile. In the current method, we made the long diameter of the ellipse match the imaging optics diameter, which resulted in the short diameter being smaller than the optics diameter. In a slightly modified approach, we tried to make the short diameter match the imaging optics diameter, which made the long diameter bigger than the aperture of the imaging optics. We then tried to carefully polish off the redundant epoxy once it was cured. The epoxy grating, however, cracked during the polishing process, and we ended up having an even smaller grating diameter than that by the current method. In yet another approach, we applied an ample amount epoxy between the imaging optics and the elastomeric stamp and introduced the UV light through the imaging optics. Since the UV light was delivered through the imaging optics, only the epoxy on the light path of the imaging optics was cured. The intensity of the UV light, however, was low at the edge of the imaging optics due to the low coupling efficiency and high internal scattering of the fiber in the imaging optics. Therefore the grating was formed only at the central portion of the imaging optics even after hours of UV curing. Use of a UV curing epoxy with a higher viscosity may reduce the spread of the epoxy along the grooves and subsequently may make the epoxy shape more circular. We can make an elastomeric stamp with multiple circular pillars. Each pillar has the grating pattern at the top, and the diameter of each pillar is same to the imaging optics diameter. This new stamp can ensure that the epoxy does not spread behind the diameter of the imaging optics and can make it easy to achieve a circular epoxy spread with a diameter same to the imaging optics diameter.

We have noticed that the edge of the cured epoxy did not replicate the grating pattern well. The presence of oxygen during the UV curing process is known to make a tacky surface of the cured epoxy and degrade the mechanical and physical properties.[24] The edge of the epoxy is exposed to surrounding oxygen while the middle part of the epoxy is sealed against oxygen by the imaging optics and elastomeric stamp, and this difference caused the lack of the grating pattern at the edge. The presence of oxygen can be mitigated by using nitrogen during the UV curing, and the oxygen inhibition can improve the epoxy curing at the edge and increase the grating area. In addition the curing speed can be increased by delivering the UV light more efficiently and/or using a higher-power UV lamp, which can improve the mechanical and physical properties of the cured epoxy at the edge.

Conclusions

We have developed a new method for fabricating SEE probes that uses soft-lithographic replica molding. The new method uses a composite elastomeric stamp to create a miniature diffraction grating at the tip of the device. Using this fabrication process, we have constructed a 500-μm-diameter SEE probe with high diffraction efficiency. The imaging results showed that the SEE probe can visualize key anatomic details of biological samples with high image contrast. The new method provides a cost-effective and reliable way of fabricating SEE probes.

The next step of this research is to test the utility of the SEE technology for various clinical applications, including fetal imaging, image-guided fetal surgery, neuro surgery, and other minimally-invasive imaging applications where the small size of the SEE probe can improve the procedure outcomes and reduce the risk of the procedure.

Acknowledgments

The authors thank Drs. Daniel Irimia and Salil Desai at BioMEMS resource center, Massachusetts General Hospital for their help on the elastomeric stamp fabrication during early stage of the research. This research was sponsored by National Institute of Health/National Institute of Biomedical Imaging and Bioengineering (Grant#

R21EB007718) and by the Office of Naval Research under award N0014-10-1-0942. R.V.M. acknowledges funding by the FP7 People program under the project Marie Curie IOF-275148. G. J. T is currently receiving research sponsorship from Canon related to the subject matter of this paper. The authors have submitted a provisional US patent application for the fabrication method described in this paper.

References

1. Ruano R, Yoshisaki CT, Salustiano EM, Giron AM, Srougi M, Zugaib M. Ultrasound Obstet Gynecol. 2011; 37:696–701. [PubMed: 21337440]
2. Deprest J, Nicolaides K, Done E, Lewi P, Barki G, Largen E, Dekoninck P, Sandaite I, Ville Y, Benachi A, Jani J, Amat-Roldan I, Gratacos E. J Pediatr Surg. 2011; 46:11–11.
3. Bauters C, Lablanche JM, McFadden EP, Hamon M, Bertrand ME. Circulation. 1995; 92:2473–2479. [PubMed: 7586347]
4. Ramee SR, White CJ, Collins TJ, Mesa JE, Murgo JP. J Am Coll Cardiol. 1991; 17:100–105. [PubMed: 1987210]
5. Thiberville L, Salaün M, Lachkar S, Dominique S, Moreno-Swirc S, Vever-Bizet C, Bourg-Heckly G. Eur Respir J. 2009; 33:974–985. [PubMed: 19213792]
6. Jacobs VR, Kiechle M, Plattner B, Fischer T, Paepke S. J Minim Invasive Gynecol. 2005; 12:359–364. [PubMed: 16036199]
7. Gazala MA, Shussman N, Gazala SA, Schlager A, Elazary R, Ponomernco O, Khalaila A, Rivkind AI, Mintz Y. J Laparoendosc Adv Surg Tech A. 2012; 22:984–988. [PubMed: 23190043]
8. Seibel EJ, Smithwick QY. Lasers Surg Med. 2002; 30:177–183. [PubMed: 11891736]
9. Lee CM, Engelbrecht CJ, Soper TD, Helmchen F, Seibel EJ. J Biophotonics. 2010; 3:385–407. [PubMed: 20336702]
10. Tearney GJ, Shishkov M, Bouma BE. Opt Lett. 2002; 27:412–414. [PubMed: 18007818]
11. Yelin D, Bouma BE, Tearney GJ. Opt Express. 2008; 16:1748–1757. [PubMed: 18542254]
12. Yelin D, Yun SH, Bouma BE, Tearney GJ. Opt Lett. 2005; 30:1794–1796. [PubMed: 16092348]
13. Yelin D, White WM, Motz JT, Yun SH, Bouma BE, Tearney GJ. Opt Express. 2007; 15:2432–2444. [PubMed: 19532480]
14. Yelin D, Bouma BE, Rosowsky JJ, Tearney GJ. Opt Express. 2008; 16:14836–14844. [PubMed: 18795020]
15. Yelin D, Rizvi I, White WM, Motz JT, Hasan T, Bouma BE, Tearney GJ. Nature. 2006; 443:765. [PubMed: 17051200]
16. Shishkov, M.; Tearney, GJ.; Bouma, BE.; Yelin, D.; Iftimia, N. United States Pat. US8145018. 2012.
17. Engel G, Genish H, Rosenbluh M, Yelin D. Biomed Opt Express. 2012; 3:1855–1864. [PubMed: 22876349]
18. Qin D, Xia Y, Whitesides GM. Nature Protocols. 2010; 5:491–502.
19. Elhadj S, Rioux RM, Dickey MD, DeYoreo JJ, Whitesides GM. Nano Letters. 2010; 10:4140–4145. [PubMed: 20843061]
20. Hua F, Sun Y, Gaur A, Meitl MA, Bilhaut L, Rotkina L, Wang J, Geil P, Shim M, Rogers JA. Nano Letters. 2004; 4:2467–2471.
21. Pokroy B, Epstein AK, Persson-Gulda M, Aizenberg J. Adv Mat. 2009; 21:463–469.
22. Gaoliang D, Ludger K, Frank P, Thorsten D, Hans-Ulrich D. Meas Sci Tech. 2005; 16:1241.
23. Stürmer H. Product Manager at GRINtech, personal communication.
24. UV Cure Adhesives. http://www.epotek.com/SSCDocs/techtips/Tech%20Tip%209%20-%20UV%20Cure%20Adhesives.pdf

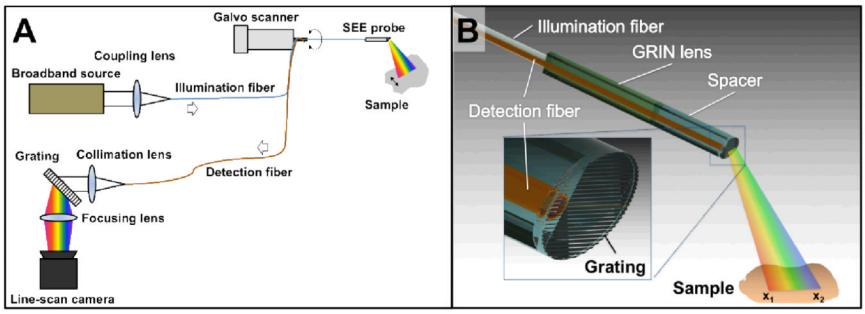

Fig. 1.
Schematics of (A) SEE system and (B) SEE probe.

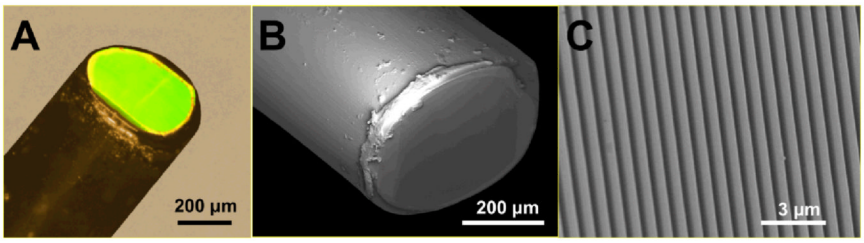

Fig. 2.
Light microscopy image (A) and SEM images (B and C) of the tip of the SEE probe.

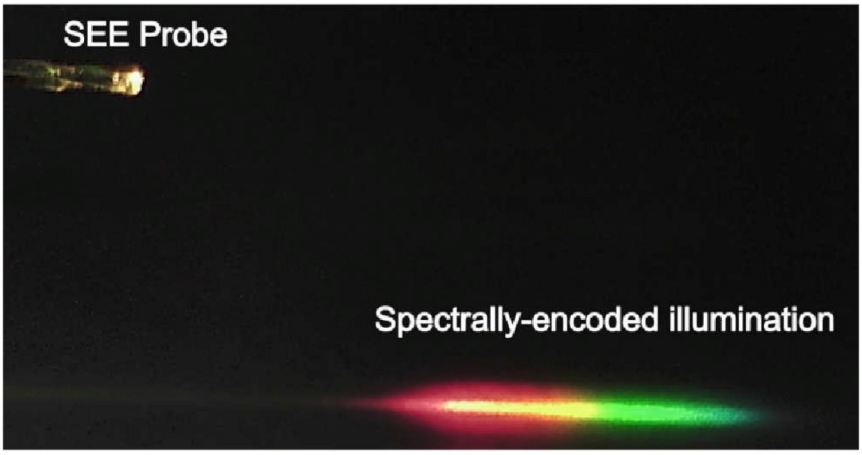

Fig. 3.
Photo of the SEE probe and spectrally-encoded illumination.

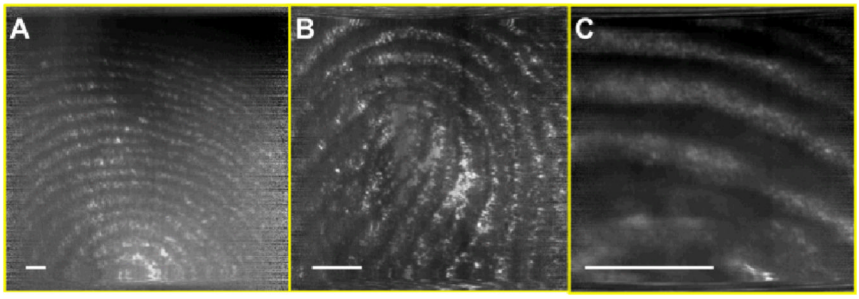

Fig. 4.
SEE images of human finger at three different working distances. Scale bar = 1mm.

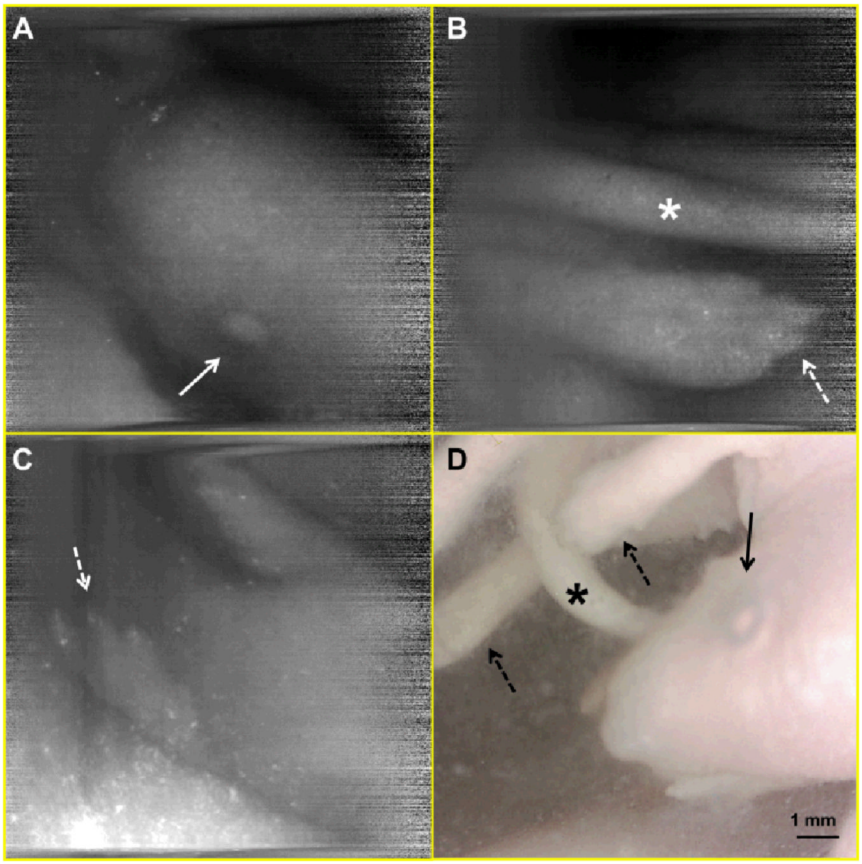

Fig. 5.
SEE images (A, B, and C) and photo (D) of mouse embryo. arrow – eye; asterisk – tail, dotted arrow – paw.